SINGULARITY TRAJECTORY ANALYSIS OF 6-SPS STEWART PLATFORM

Ruixia Li[1,], Fenxia Li[2]*
[1]Department of Biomedicine Engineering, Changzhi Medical College, Changzhi 046000, China
[2]Numerical Control Engineering Department, Shanxi Institute of Mechanical and Electrical Engineering, Changzhi 046011, China

Abstract - This paper presents an analysis of the singularity configuration trajectory of a symmetric 6-SPS Stewart platform, a 6-DOF parallel mechanism with three translational and three rotational degrees of freedom (3T3R). The mechanism consists of a fixed base, a moving platform, and six identical limbs. The inverse kinematics of the parallel mechanism is first calculated and its velocity equation in terms of Jacobian matrix is derived in detail, which is important to the singularity configuration analysis. A polynomial form of the singularity trajectory is also deduced. Three kinds of singularities are presented in sequence. A graphical representation of the complete singularity trajectory of the parallel mechanism is illustrated with some numerical examples. The analytic results show that the algorithm presented in this paper allows the determination of the singularity configuration trajectory of the parallel mechanism, which is alternative available method to the other parallel mechanism.

Keywords: 6-SPS Stewart platform; Jacobian matrix; Singularity configuration; Singularity Trajectory.

1. Introduction

Compared with the traditional serial mechanism, the parallel mechanism has the characteristics of high stiffness, high control precision and high loading capacities, so it can be widely used in high-precision machining tools (e.g., five-axis CNC milling machines), flight simulators, medical robotics, and so on[1-3]. However, the singularity configurations of parallel mechanisms are critical poses characterized by either the loss of some degrees of freedom, the gain of some extra degree of freedom or the loss of stiffness. The determination of singularity configurations is thus a central issue in robotics due to their major effect on the robot performance [4]. So it is very important to be able to predict singularity configurations for a given kinematic architecture. Recently, singularity configurations have received considerable attentions from researchers due to the limitations in the engineering application.

Singularity configurations are inherent to the parallel mechanism, which is undesirable in mechanism operation process for both motion and force control. In order to achieve effective application of the parallel mechanism, the singularity configuration of the parallel mechanism should be one of main concerns in the analysis and design of the parallel mechanism, and also is one of the important problems in kinematics problem of the parallel mechanism. A large number of researches have been done by domestic and foreigner scholars on this issue. For example, Gosselin et al. used the Grassmann geometry to analyze the singularity, and the results illustrated that all singularities can be avoided by exploiting the kinematic redundancy [5]. In [6], the singularity of the series-parallel mechanism is defined by the input and output velocity equations, and the conditions for the existence of the singularity configuration are studied by the principle of line bundle and algebra, respectively. The singularity including constraint, input transmission and output transmission performance is investigated by the motion-force transmission performance indices in [7].

The singularity of the 3-PSR-O parallel mechanism was carried out based on the geometrical constraints, including six singularity boundaries, and a feature boundary was obtained by integrating the six singularity boundaries [8]. Amine et al. [9] used the Jacobian matrix to analyze the singularity configuration in terms of the Grassmann-Cayley algebra and Grassmann geometry method.

https://doi.org/10.17683/ijomam/issue23

Liu et al. [10] presented a new approach for singularity analysis of parallel mechanism by taking into account motion/force transmissibility, which can measure the closeness between a pose and a singularity configuration. In [11], various singularity configurations were identified by analyzing screw dependency in the Jacobian matrix, and the singularity-free workspace was further depicted. According to the classification given in [12], there are three types of singularities for closed-loop mechanisms, based on the properties of the Jacobian matrices of the chain. The second type of singularity is the focus of our study, i.e., the determinant of the instantaneous direct kinematics matrix is equal to zero. Generally, domestic scholars use the method of instantaneous velocity and matrix analysis to determine the singularity configuration of the parallel mechanism. Most of these methods are based on algebraic methods to classify and define singularity configurations, or to calculate some specific properties, but the rich geometric properties contained in the singularity configuration are rarely involved.

In this work, a 6-SPS Stewart platform is studied. Section 2 briefly introduces the structure of the parallel mechanism, and a complete kinematics model including the inverse and forward Jacobian matrix was derived. Section 3 singularity configurations analysis is performed with the determinant of the Jacobian matrix. In section 4 numerical examples are then introduced to obtain graphical representations of the singularity configuration trajectories. Conclusions are finally drawn in Section 5.

2. Kinematics Analysis

2.1 Structure of the Parallel Manipulator

In this paper, the following symbols are used consistently:

a--radius of the circle on which base joints are located (mm);

b--radius of the circle on which platform joints are located (mm);

$\boldsymbol{A}_i$--spherical joint centers on the moving platform (i=1,...,6);

$\boldsymbol{B}_i$--spherical joint centers on the fixed base (i=1,...,6);

$\boldsymbol{l}_i$--ength of the i-th limb (mm);

R-- rotation matrix from the moving frame to the fixed frame.

Figure 1 illustrates the prototype of the proposed 6-DOF parallel mechanism, which consists of a fixed base, a moving platform, and six variable active limbs (SPS) with identical topology [13]. The 6-SPS parallel mechanism interconnection between the moving platform and the fixed base, which S stands for spherical joint, and P for the prismatic joint which is actuated independently by an AC permanent magnet servo-motor via a synchronous belt and a ball screw. An electrical spindle is mounted on the platform to implement high-speed milling. The schematic of the mechanism is shown in Figure 2, whose points of kinematic joints attached to the moving platform and the fixed platform are denoted by $\mathbf{A}_1$, $\mathbf{A}_2$, $\mathbf{A}_3$, $\mathbf{A}_4$, $\mathbf{A}_5$, $\mathbf{A}_6$ and $\mathbf{B}_1$, $\mathbf{B}_2$, $\mathbf{B}_3$, $\mathbf{B}_4$, $\mathbf{B}_5$, $\mathbf{B}_6$, respectively. All the spherical joints are uniformly distributed, and link lengths are represented by l_1, l_2, l_3, l_4, l_5, l_6.

Figure 1: The prototype of the 6- DOF parallel mechanism

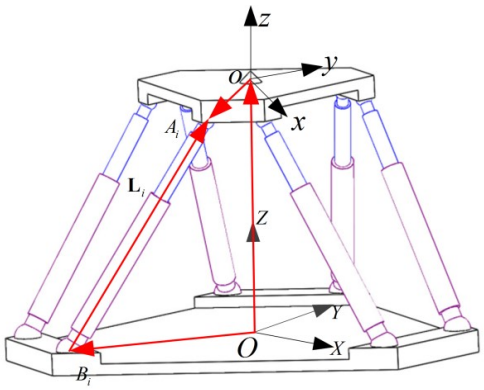

Figure 2: The schematic of 6-SPS parallel mechanism

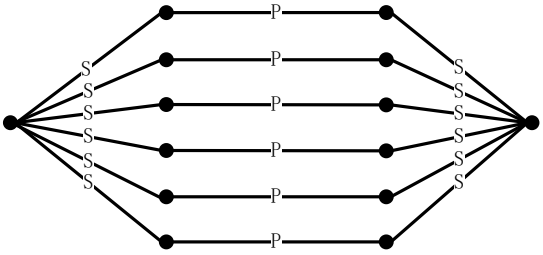

Figure 3: Topology diagram of the mechanism model

Figure 3 provides a graphical integration of the parallel mechanism, where point represents mechanism components, side represent of kinematic

joints, S represents the spherical joint, and P represents the prismatic joint, the topological structural can be obtained by merging the points in Figure 4 as follows:

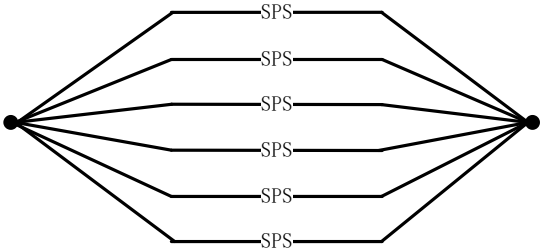

Figure 4: Topological scaling of the mechanism model

Therefore, the Stewart parallel mechanism is also called as the 6-SPS parallel mechanism. The topology number of the closed loops of the mechanism is five.

2.2 The Geometric Properties of the Mechanism

For the purpose of analysis, the kinematic schematic structure of the proposed 6-DOF parallel mechanism is depicted in Figure 2. Suppose that the center of the S joint located on the base and moving platform are distributed on the circles with radius a and b respectively. A fixed coordinated frame O-XYZ is attached to the central point O of the base and a moving coordinate frame o-xyz is attached on the platform. Let x-axis point to A1 and X-axis point to the B1. The Cartesian coordinates of the moving platform are defined by the position o = $(x, y, z)^T$ in the fixed frame, where x, y, z represent translational displacements along the X, Y, Z axes, respectively. This vector is used to calculate non-singularity configurations and analyze orientation-singularities.

The orientation of the moving platform is represented by standard Z_ψ-Y_θ-X_φ Euler angles, where φ,θ,ψ denote rotations about the X, Y, and Z axes, respectively. the translation rotation R with respect to the fixed coordinate system can be expressed as shown in Equation (1).

$$\begin{aligned}\boldsymbol{R} &= Rot(z,\psi)Rot(y,\theta)Rot(x,\varphi)\\ &= \begin{bmatrix}\cos\psi & -\sin\psi & 0\\ \sin\psi & \cos\psi & 0\\ 0 & 0 & 1\end{bmatrix}\begin{bmatrix}\cos\theta & 0 & \sin\theta\\ 0 & 1 & 0\\ -\sin\theta & 0 & \cos\theta\end{bmatrix}\begin{bmatrix}1 & 0 & 0\\ 0 & \cos\varphi & -\sin\varphi\\ 0 & \sin\varphi & \cos\varphi\end{bmatrix}\\ &= \begin{bmatrix}\cos\psi\cos\theta & \cos\psi\sin\theta\sin\varphi-\sin\psi\cos\varphi & \sin\psi\sin\varphi-\cos\varphi\sin\theta\cos\varphi\\ \sin\psi\cos\theta & \cos\psi\cos\varphi-\sin\psi\sin\theta\sin\varphi & \cos\psi\sin\theta\cos\varphi-\cos\psi\sin\varphi\\ -\sin\theta & \cos\theta\sin\varphi & \cos\theta\cos\varphi\end{bmatrix}\end{aligned} \quad (1)$$

The generalized coordinates $\boldsymbol{q}=[x,y,z,\varphi,\theta,\psi]^T$ are selected as parameters, where q represents the pose vector of the moving platform, so that the positions and orientations of the arbitrary point in the fixed coordinate system can be written as shown in Equation (2).

$$\boldsymbol{l}_i^2 = \left\|-\boldsymbol{OB}_i + \boldsymbol{R}\times\boldsymbol{oA}_i + \boldsymbol{Oo}\right\|^2 \quad (2)$$

Differentiating Equation (3) with regard to time, yields the following relationship.

$$\begin{aligned}l_i\dot{i}_i &= \left((oA_i-OB_i)^T\dot{O}o + (oA_i-OB_i)^T\omega\times RoA_i\right)\\ &= \left[(oA_i-OB_i)^T, (RoA_i\times(oA_i-OB_i))^T\right]\begin{bmatrix}\dot{O}o\\ \omega\end{bmatrix}\\ &= \left[(oA_i-OB_i)^T, (RoA_i\times(oA_i-OB_i))^T\right]\dot{q}\end{aligned} \quad (3)$$

The input joint velocity and the end-effector output velocity of the Stewart can be expressed as shown in Equation (4).

$$C\dot{q} = D\dot{l} \quad (4)$$

Then the two Jacobian matrix equations are derived as shown in Equation (5)-(7), where C and D denote the inverse and forward Jacobian matrices, respectively.

$$\boldsymbol{C}=\begin{bmatrix}c_1 & c_2 & c_3 & c_4 & c_5 & c_6\end{bmatrix}^T \quad (5)$$

$$\boldsymbol{D}=diag(l_1,l_2,l_3,l_4,l_5,l_6) \quad (6)$$

$$c_i=\left[\left(\boldsymbol{oA}_i-\boldsymbol{OB}_i\right)^{\mathrm{T}}, \left(\boldsymbol{RoA}_i\times\left(\boldsymbol{oA}_i-\boldsymbol{OB}_i\right)\right)^{\mathrm{T}}\right], \quad i=1,2,\ldots,6 \quad (7)$$

So far, the velocity equations represent the linear velocity mapping between the joint space and Cartesian operation space. They are particularly important because they characterize the kinematic accuracy of the mechanism and allow determining the singularities. Therefore, the singularity configuration of the Stewart parallel manipulator can be analyzed by evaluating the determinants of the inverse (C) and forward (D) Jacobian matrices.

All symbols are defined with units: lengths in mm, angles in rad, velocities in mm/s and rad/s.

3. Singularity Trajectory Analysis of the Platform

In the configuration space of the parallel mechanism, in general, the singularity configuration is not a single point, but a set of curves or high-dimensional surfaces (hyper-surfaces) called singularity trajectory. Because singularity may lead to a loss of the controllability and degradation of the stiffness of the parallel mechanism, the analysis of

parallel mechanism needs to pay considerable attention.

To determine if the Stewart platform has a singularity trajectory in a given workspace, inhere, we consider the forward and inverse Jacobian matrix between the speed input and output equation of the Stewart platform firstly. According to the classification method proposed by Gosselin and Stonge [14], the three kinds of singularities of the parallel mechanism can be obtained.

In order to visually represent singularity trajectories in three-dimensional space, and also to simplify the algebraic process of the six positions and orientations variables of the Stewart platform as constants, and then use the Matlab software to solve them by programming. The analytic expression of the Jacobian matrix determinant containing the other three variables is equal to the zero-time equation, which is the expression of the singularity trajectory of the Stewart platform with three pose variables. On this basis, the singularity trajectory of the Stewart platform is represented in the three dimensional space by a numerical programming.

3.1 Inverse Kinematic Singularity Configuration

At this point, the determinant of D is zero, that is, li=0 (one or a few values in 1-6 limbs), but in fact, because actuator lengths of the Stewart platform are constrained within a certain range lmin<li<lmax, that is, the singularity configuration does not occur in the workspace. However, at the boundary of the workspace, when one or more limbs are fully extended or contracted, the platform enters an inverse kinematic singularity configuration and loses one degree of freedom. That is, regardless of the speed of a given actuator, the upper platform cannot be made to produce velocity in that direction.

3.2 Forward Kinematic Singularity Configuration

At this issue, the forward kinematic singularity occurs when the determinant of C is zero. That is, the moving platform may have non-zero velocity even if all actuators are stationary. At this time, even if a great force is given to the actuator, the external force on the moving platform cannot be overcome, namely, the local stiffness of the parallel manipulator is zero, which is very dangerous for the Stewart platform. When the platform is in the vicinity of the singularity configuration, the gravity generated by the load will perform a large force or moment on the connecting joints and the actuators, and even damage the mechanical components. Therefore, for the Stewart platform, it is very important to judge whether there is a forward singularity in the workspace. It is very difficult to research this problem.

3.3 Combined Singularity Configuration

At this case, the determinant of C and the determinant of D are both zero. According to a simple analysis, when the moving platform and the fixed platform of the Stewart platform are congruent polygons, and when all the actuator lengths reach their maximum or minimum values, a combined singularity will occur under this circumstance. At this point, even if all the limbs are locked, the moving platform of the Stewart can still move around the spherical center of the base. The combined singularity is actually related to the special structure of the Stewart platform. It is a kind of structural singularity, which can be easily avoid when the structure of the platform is designed.

Since it is impossible to draw a singularity trajectory map with six positions and orientations variables in three dimensional spaces, any three variables of the six pose variables are set as constants, and the algebraic method is used to solve the determinant of the velocity Jacobian matrix through Matlab software. Since visualizing a 6-dimensional singularity locus is infeasible, we fix three pose variables as constants and solve the Jacobian determinant equation for the remaining three using MATLAB R2023a. We can get the analytical expressions of the determinant containing the other three pose variables. Let the expression be zero, and the singularity trajectory equation of the Stewart platform with three pose variables will be obtained. The Jacobian matrix expression depends only on joint coordinates (OAi, OBi) and rotation matrix R, enabling generalizable singularity analysis.

For example, assuming the three variables are constants, then solve the expression of the determinant of the Jacobin matrix C, and finally obtain the analytical expression of the singularity trajectory equation with positional variables, shown in Equation (8).

$$\begin{aligned} S(x,y,z) &= s_1x^3 + s_2x^2y + s_3x^2z + s_4xy^2 + s_5xyz \\ &+ s_6xz^2 + s_7y^3 + s_8y^2z + s_9yz^2 + s_{10}z^3 + s_{11}x^2 \\ &+ s_{12}xy + s_{13}xz + s_{14}y^2 + s_{15}yz + s_{16}z^2 + s_{17}x \\ &+ s_{18}y + s_{19}z + s_{20} = 0 \end{aligned} \tag{8}$$

Equation (8) is a third-order polynomial in x, y, z, where coefficients depend on structural parameters (a, b) and Euler angles (φ,θ,ψ). In the same way, the analytic expression of the singularity trajectory equation with any three pose variables and three other pose variables can be obtained by the singularity trajectory analysis method proposed

above. In view of the complexity of the expression, it is not explicitly given here. The singularity trajectory of the Stewart platform can be drawn in three-dimensional space on the basis of numerical analysis, as demonstrated in Section 4.

4. Singularity Trajectory Examples of the Stewart platform

The singularity trajectory of the Stewart platform can be depicted in three dimensions by resorting to the trajectory equation in section three. The Table I below gives the coordinates of the center points of the upper and lower joints of the parallel mechanism. The scale parameters of the parallel mechanism are radii of the moving platform a=100 mm and the fixed platform b=200mm. According to this parameter, it is simple to solve the inverse kinematic singularity and the combined singularity of the Jacobian matrix C and D. It is proved that the Stewart mechanism does not have inverse kinematic singularity and combined singularity in the reachable workspace. Therefore, the forward kinematic singularity trajectory is solved mainly according to the method described in section.

Table 1: The joint coordinates of the Stewart platform

i	OA_i	OB_i
1	(-25.88, 96.59,198.6)	(-141.42,141.42, 0)
2	(25.88,96.59,198.6)	(141.42,141.42, 0)
3	(96.59,-25.88,198.6)	(193.19,51.76, 0)
4	(70.71,-70.71,198.6)	(51.76,-193.19, 0)
5	(-70.71,70.71,198.6)	(-51.76,-193.19, 0)
6	(-96.59,-25.88,198.6)	(-193.19,51.76, 0)

The singularity configurations of the proposed parallel mechanism with specific geometric parameters are plotted based on the above-mentioned method.

4.1 Position Singularity Trajectory

According to the method described above, three angles variables are constants. In this example, assuming $[\varphi,\theta,\psi]^T=\left[-15^\circ,26^\circ,-32^\circ\right]^T$, so the singularity trajectory equation S(x,y,z)=0 can be obtained. Let the range of the three variables x, y, and z be taken as (-800,800), the numerical solution of the corresponding position singularity trajectory can be demonstrated in Figure5.

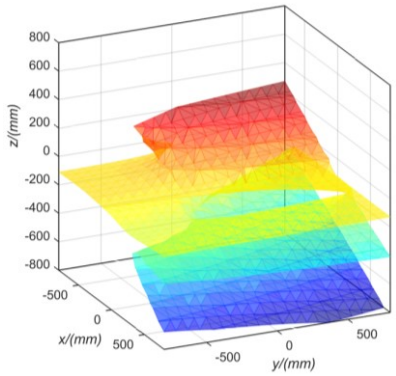

Figure 5: Position singularity configuration for specific orientations

4.2 Orientation Singularity Configuration

Let $[x,y,z]^T=[0,0,240]^T$, the singularity configuration trajectory equation $S(\varphi,\theta,\psi)=0$ can be obtained with constant position coordinate variables. The value range of the three variables $\varphi,\theta,\psi \in (-\pi/2,\pi/2)$, the orientation singularity trajectory is illustrated in Figure 6, showing a complex angular distribution.

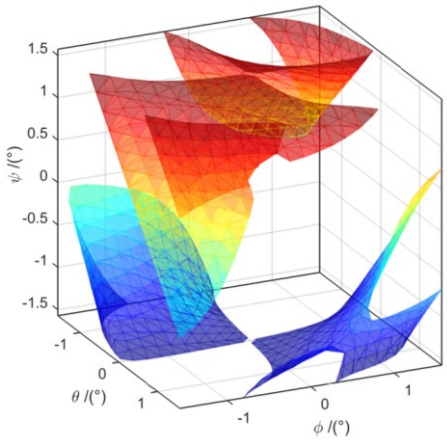

Figure 6: Orientation singularity configuration for specific position

4.3 Combined Singularity Configuration

In order to research the singularity in different positions and orientations, two combinations are constructed respectively.

In the first case, under the conditions that $[z,\theta,\psi]^T=\left[220,30^\circ,-27^\circ\right]^T$, the singularity trajectory equation $S(x,y,\varphi)=0$ can be obtained, and the remaining three variables are in the range $x,y\in(-800,800)$, $\varphi\in(-\pi/2,\pi/2)$ respectively, and the corresponding singularity trajectory can be obtained as shown in Figure 7 (a).

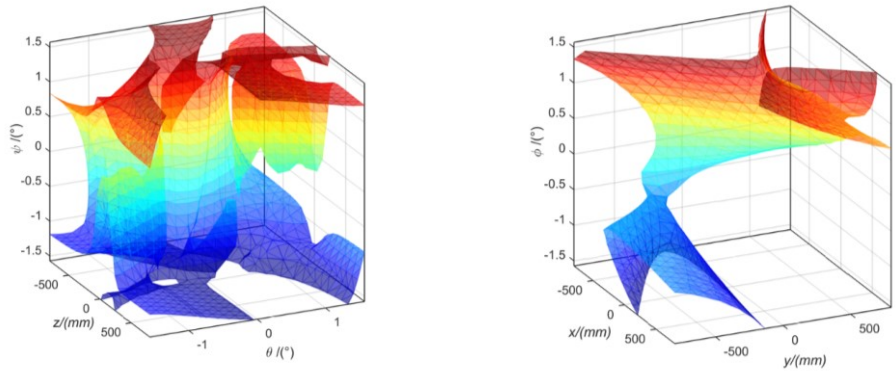

(a) Under the first combination (b) Under the second combination

Figure 7: Combined singularity trajectory

In the second case, with the consideration of the conditions that $[x,y,\varphi]^T=[0,40,-20^\circ]^T$, the singularity trajectory equation $S(z,\theta,\psi)=0$ is obtained, and the remaining three variables are in the range of $z\in(-800,800)$, $\theta,\psi\in(-\pi/2,\pi/2)$ respectively, and the corresponding singularity trajectory can be numerically depicted in Figure 7 (b).

It can be seen from the singularity trajectory depicted above that the forward kinematic singularity of the Stewart platform is very complex. It is a hyper-surface distributed in the workspace of the Stewart platform, and the workspace is divided into several locally connected regions, which limits the normal use of the platform, such a rich singularity trajectory also makes the singularity path planning of the Stewart platform very complicated. Notably, the hollow structure of the singularity trajectory (Figs. 5-7) indicates that restricting the workspace to inner regions can avoid forward singularities, which provides a theoretical basis for singularity-free structural design and workspace optimization.

5. Conclusions and Future Works

Singularity of the 6-SPS parallel mechanism is analyzed using the analytic method presented in this paper. Based on the Jacobian matrix, the analytic singularity configuration trajectory equations are obtained and the three kinds of singularities of the parallel mechanism are analyzed. The main contributions of this paper are summarized as follows:

(1) The polynomial form of the singular trajectory equation is proposed to overcome the limitation of the traditional isolated singular point analysis.

(2) The 3D trajectory visualization is realized to show the distribution characteristics of the singular surface in the workspace. The parallel mechanism can be avoided the singularities in the workspace by limit the design structural parameters.

(3) A prototype implementation validating the kinematic model. Future work will focus on dynamic analysis, real-time singularity avoidance control, and comparison with screw theory/Grassmann-Cayley algebra methods.

References

[1] G. Spagnuolo, M. Malosio, T. Dinon, and L. M. Tosatti. “Analysis and synthesis of LinWWC-VSA, a Variable Stiffness Actuator for linear motion”, Mechanism and Machine Theory, 2017, vol.110, pp.85-99.

[2] Y. Shneor, V. T. Portman. "Stiffness of 5-axis machines with serial, parallel, and hybrid kinematics: Evaluation and comparison", CIRP Annals, 2010, vol. 59, no.1, pp. 409--412.

[3] H. Xie, K. M. Zhang, and Q. Li. "The positive solution of a 5-strut parallel machine tool with joint rings", Journal of Intelligent and Robotic Systems, 2012, vol. 66, no.4, pp.429-441.

[4] H. Y. Chuang, K. H. Chien. “Analysis of workspace and singularity of a slide equilateral triangle parallel manipulator”, Journal of System Design and Dynamics, 2007, vol. 1, no. 4, pp. 724-735.

[5] C. Gosselin, L. T. Schreiber. “Kinematically redundant spatial parallel mechanisms for singularity avoidance and large Orientational workspace”, IEEE Transaction on Robotics, 2016, vol.32, no. 2, pp. 286-300.

[6] J. P. Merlet. “Singular configurations of parallel manipulators and Grassmann geometry”, the International Journal of Robotics Research, 1989, vol. 8, no. 5, pp. 45–56.

[7] F. G. Xie, and X. J. Liu. “Analysis of the kinematic characteristics of a high-speed parallel robot with Schönflies motion: Mobility, kinematics, and singularity”, Frontiers of Mechanical Engineering, 2016, vol.11, no. 2, pp. 135-143.

[8] Y. Cao, C. Gosselin, H. Zhou, and P. Ren. “Orientation-singularity analysis and orientationability evaluation of a special class of the Stewart–Gough parallel manipulators”, Robotica, 2013, vol. 31, no. 8, pp. 1361-1372.

[9] M. T. Amine, S. C. Masouleh, and P. Wenger. "Singularity analysis of 3T2R parallel mechanisms using Grassmann–Cayley algebra and Grassmann geometry", Mechanism and Machine Theory, 2012, vol. 52, pp. 326-340.

[10] X. J. Liu, C. Wu, J. S. Wang. "A new approach for singularity analysis and closeness measurement to singularities of parallel manipulators", Journal of Mechanisms and Robotics, 2012, vol.4, no. 4, pp. 1-10.

[11] Y. F. Zhuang, D. M. Gan. "Unified singularity modeling and reconfiguration of 3RTPS metamorphic parallel mechanisms with parallel constraint screws", Advances in Mechanical Engineering, 2014, vol. 15, pp.1-12.

[12] C. Gosselin, J. Angeles. "Singularity analysis of closed-loop kinematic chains", IEEE Transaction on Robotics and Automation, 1990, vol.6, no.3, pp.281-290.

[13] R. X. Li, and F. X. Li, "Workspace performance investigation of a multi-dof parallel robot manipulator," International Journal of Engineering and Technology, 2019, vol. 11, no. 1, pp. 1-5.

[14] B. M. Stonge, and C. Gosselin. "Singularity analysis and representation of the general gough-stewart platform", The International Journal of Robotics Research, 2000, vol.19, no.3, pp.271-288.